GEUS Bulletin | Geological Survey of Denmark and Greenland

RESEARCH ARTICLE

The sedimentology and depositional environments of the Bastians Dal and Muslingebjerg formations: evidence for the earliest phases of Jurassic rifting in North-East Greenland

Steven D. Andrews*[1], Henrik Vosgerau[2], Jørgen A. Bojesen-Koefoed[2]

[1]University of the Highlands and Islands, Inverness, UK. [2]Geological Survey of Denmark and Greenland (GEUS), Copenhagen, Denmark

Abstract

The aim of this study is to elucidate the character of the earliest phases of Jurassic rifting in North-East Greenland. To achieve this, detailed sedimentological analysis and geological mapping were undertaken on the outcrops of central Kuhn Ø (74°53'55"N,20°20'56"W). In this region the basement is overlain by the fluvial Bastians Dal Formation (Middle Jurassic) which is, in turn, overlain by the coal-bearing Muslingebjerg Formation. A maximum thickness of 140 m is calculated for the Bastians Dal Formation and mapping of stratal geometries demonstrates thinning to both the north and south, confirming that these deposits infill a palaeovalley. Predominantly south-westward palaeocurrent orientations are observed and likely reflect the orientation of the palaeovalley (NE–SW). The overlying Muslingebjerg Formation displays significant lateral variations in thickness as well as facies, thickening from a 5-m-thick coal seam in the north to 50 m in the south. Southern outcrops include two intervals of fine-grained sandstones displaying low-angle and trough cross-bedding some of which contain suggestions of tidal bundling. The arrangement of facies suggests that coal formation occurred in both fluvial- and shallow-marine (tidal?) environments. Coals are similar to those described elsewhere from the Muslingebjerg Formation and display subtle differences consistent with variable degrees of marine influence. Mapping demonstrates the presence of an NE–SW-oriented bounding fault in the south of the region into which the Muslingebjerg Formation thickens. This likely also controlled the orientation of the underlying NE–SW-aligned palaeovalley and is oblique to the proposed overall N–S orientation of faulting related to rifting through the Mid to Late Jurassic. Instead, these alignments resemble those that define pre-Jurassic phases of rifting and may therefore indicate a transitional phase of tectonism. Faulting on a similar alignment can be traced SW, cutting Lindeman Fjord and following the valleys east of the A. P. Olsen Land plateau.

***Correspondence:** *steven.andrews914@gmail.com*
Received: 05 Feb 2022
Accepted: 16 Jul 2022
Published: 25 Aug 2022

Keywords: North-East Greenland, Jurassic, Tectonics, Coal, Fluvial

Abbreviations:

HI: hydrogen index
HST: highstand systems tract
OI: oxygen index
PI: production index
TC: total carbon
TOC: total organic carbon
Tmax: temperature of maximum pyrolysate-yield
TS: total sulphur
TST: transgressive systems tract
VR: vitrinite reflectance

Edited by: Mette Olivarius (GEUS, Denmark).

Reviewed by: Tiffany Playter (University of Alberta, Canada), Mihai Emilian Popa (University of Bucharest, Romania).

Funding: See page 19

Competing interests: See page 19

Additional files: See page 19

Introduction

Alsgaard *et al*. (2003) discovered fluvial deposits in the central part of the island Kuhn Ø and described the succession as being 100–150 m thick and infilling a valley system incised into the crystalline basement. They formally defined the succession as a formation and named it after the valley Bastians Dal, an E–W-trending valley in western central Kuhn Ø (Higgins 2010) where the fluvial deposits were found. Their fieldwork was concentrated to the northern part of Bastians Dal where the fluvial deposits are overlain by a *c*. 5-m-thick succession of the coal-bearing Muslingebjerg Formation. Overlying shallow-marine sandstones of the Pelion Formation mark the drowning of the valley fill and the adjacent basement peneplain (Alsgaard *et al*. 2003). The ages of the Bastians Dal and Muslingebjerg formations are not well constrained. The former was assigned a general Middle Jurassic age by Alsgaard *et al*. (2003) based on its palynological content (Fig. 1). Fragments of the ammonite *Arcticoceras* cf. *ishmae* collected from the basal part

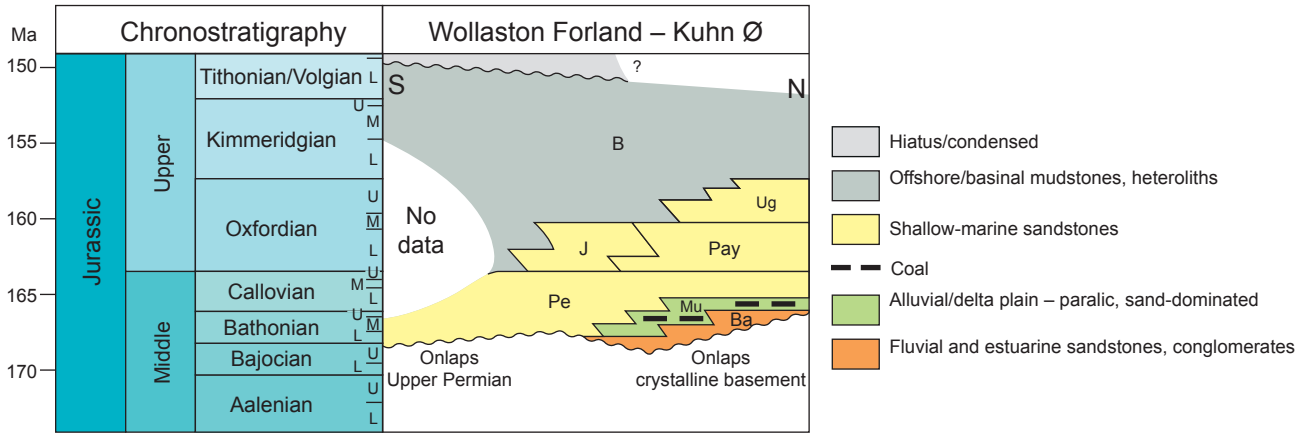

Fig. 1 Jurassic stratigraphy of Kuhn Ø. Modified from Surlyk *et al*. (2021). **Ba**: Bastians Dal Formation. **Mu**: Muslingebjerg Formation. **Pe**: Pelion Formation. **Pay**: Payer Dal Formation. **J**: Jacobsstigen. **Ug**: Ugpik Ravine Member. **B**: Bernbjerg Formation.

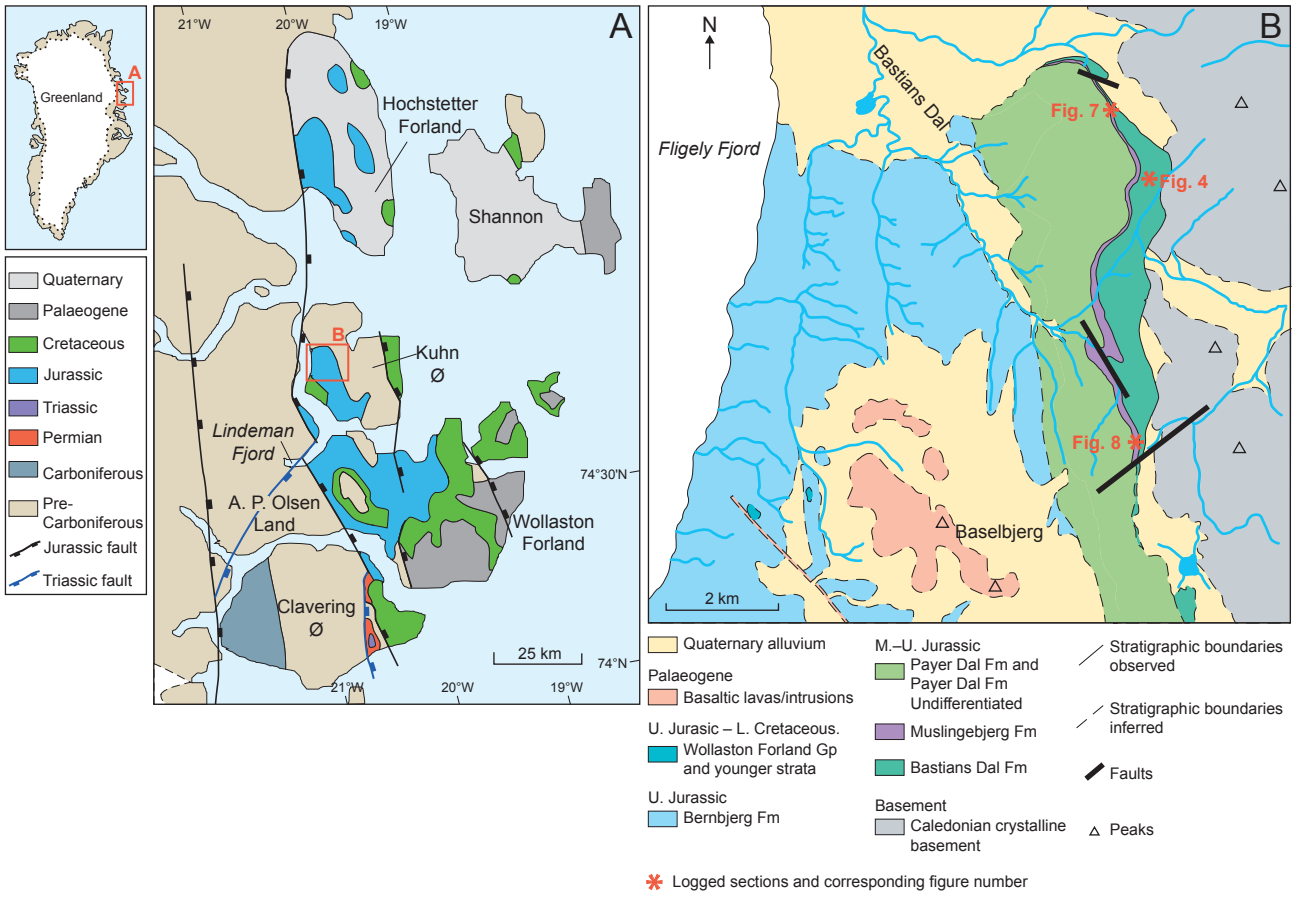

Fig. 2 Location and geology map. **(A)** Overview of the region, based on Koch and Haller (1971). **(B)** Detailed geological map of the study region, modified from Alsgaard *et al.* (2003, based on Koch & Haller (1971)) and using data collected during field mapping that formed part of this study. **U**: Upper. **M**: Middle. **L**: Lower.

of the Pelion Formation in northern Wollaston Forland (P. Alsen, personal communication 2022) indicate that the Bastians Dal and Muslingebjerg formations are no younger than the Middle Bathonian. However, the boundary with the Pelion Formation may be largely diachronous (younging towards north) as strata overlying the highest coal bed of the Muslingebjerg Formation on Hochstetter Forland contain dinoflagellate cysts suggesting the upper Callovian *P. athleta* ammonite zone (Piasecki & Stemmerik 2004).

The current study presents observations from outcrops covering the entire Bastians Dal area (74°53′55″N,20°20′56″W; Fig. 2), augmented with photogrammetrical data (Fig. 3) and analysis of coal samples and organic residues identified within sandstone samples. These new data shed further light on the

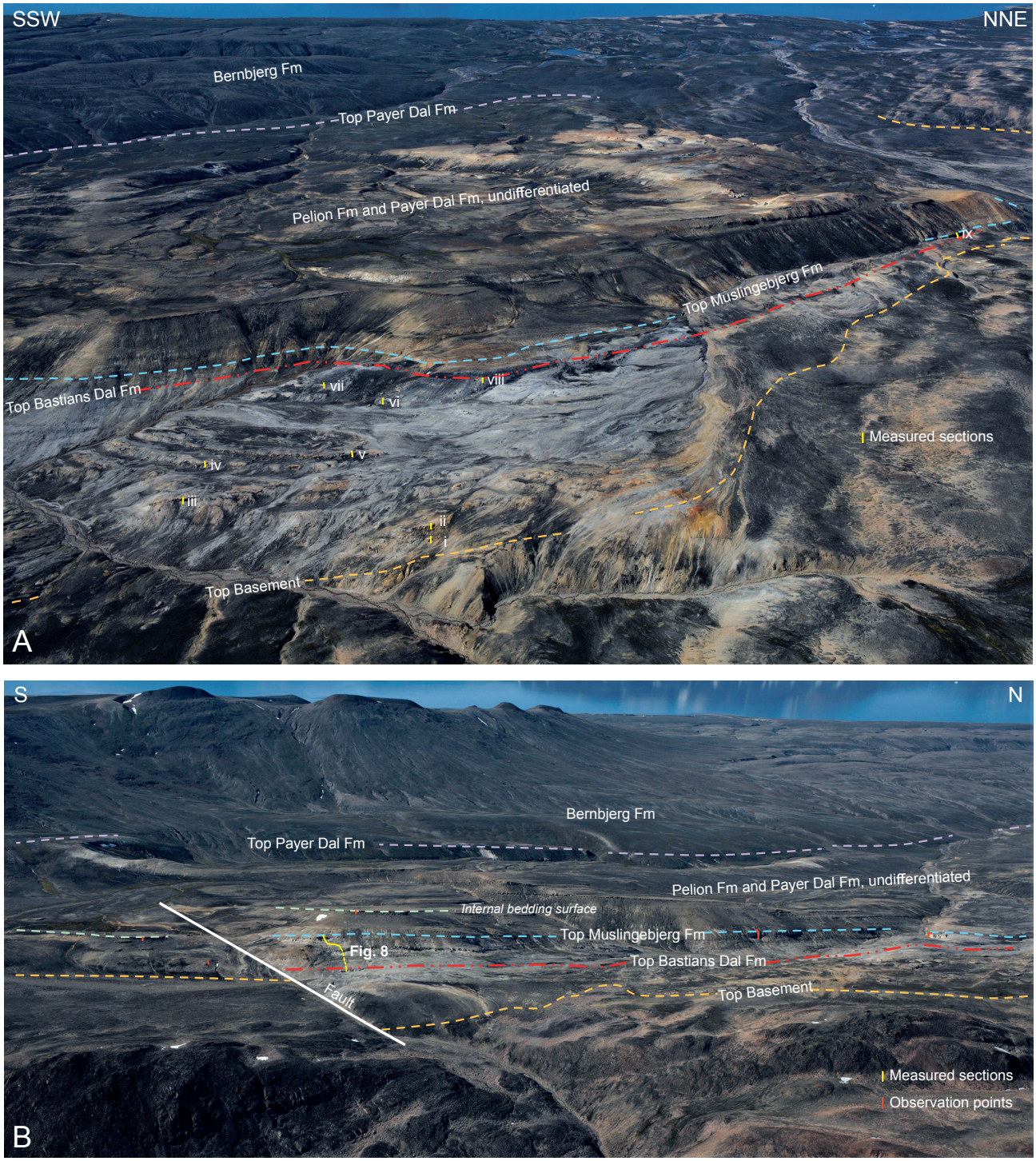

Fig. 3 Photogrammetric overview of (**A**) the northern (Bastians Dal north) and (**B**) the southern (Bastians Dal south) areas of the study region. The locations of key observations and logged sections are indicated, along with the stratigraphic boundaries identified during this study. The numbering (**i–ix**) of logged sections in A relates to those illustrated in Figs 4 and 7.

architecture, sedimentology and depositional environments of the Bastians Dal and Muslingebjerg formations and the sequence of infilling of the NE–SW-orientated palaeovalley. The orientation of this palaeovalley and associated faulting are thought to relate to a transitional phase of rift orientation between Triassic and Jurassic rifting events. The new data also reveal that the Muslingebjerg Formation expands in thickness from the *c*. 5 m in northern Bastians Dal to as much as *c*. 50 in the south. Here, coal beds are, in places, intercalated with fine-grained sandstones showing signs of tidal influence and resembling the overlying marine Pelion Formation. At the base of one of the coal beds, oily slicks were observed in out-seeping water, and analysis of the coal samples suggests that they may have acted as a source to the bitumen found within the sandstone pore systems.

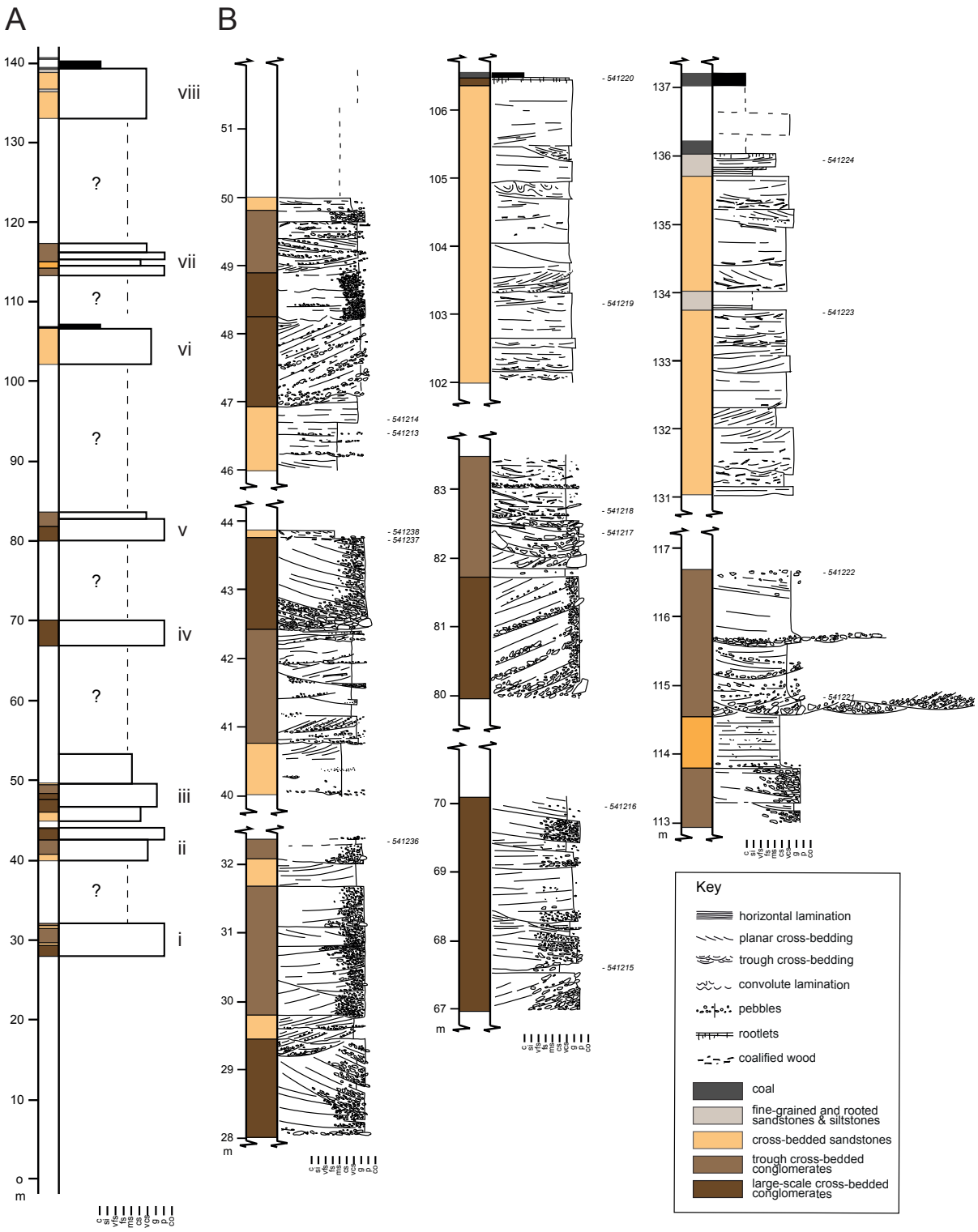

Fig. 4 Summary log through the Bastians Dal Formation (**A**) and detailed logs of the well exposed sections (**B**). The general position of the composite section is indicated in Fig. 2. Positions of the individual detailed logs, numbered **i–viii,** are provided in Fig. 3A. Relative positions as indicated on the summary log were calculated using photogrammetry. Samples collected from these sections are numbered to the right of the logs.

Geological setting

The Bastians Dal and Muslingebjerg formations form the basal part of the Middle–Upper Jurassic early syn-rift succession, which is up to 1 km thick in the Kuhn Ø region. This succession consists of large-scale, backstepping sedimentary units separated by major drowning surfaces, reflecting an overall stepwise northwards transgression. Deposition took place on the hanging wall of fault blocks within the Wollaston Forland Basin, which formed a rift-controlled embayment situated on the western margin of the N–S-trending rift complex between Greenland and Norway. The fault blocks were up to *c.* 40 km wide

and slightly tilted towards west-south-west. Towards the east, elevated fault-block crests formed elongated islands or peninsulas, which broadened and were attached to the mainland to the north. Regional sediment transport was overall axial from the north towards the south down a low-gradient basin floor (Surlyk 1977, 1990, 1991; Surlyk & Clemmensen 1983). Rifting culminated in the early Volgian – Early Ryazanian with major block faulting, tilting of blocks and the formation of halfgraben (Surlyk 1978).

Vischer (1943) and Maync (1947, 1949) were the first to describe the tectonic style and stratigraphy of Jurassic tilted fault blocks in the Wollaston Forland Basin. A number of succeeding studies focused on the sedimentary environments, lithostratigraphy and sequence stratigraphy of the early syn-rift succession (e.g. Clemmensen & Surlyk 1976; Petersen *et al*. 1998; Petersen & Vosgerau 1999; Vosgerau *et al*. 2000; Alsgaard *et al*. 2003; Surlyk 2003; Surlyk & Korstgård 2013; Surlyk *et al*. 2021).

Methodology

Field observations (August 2018) and sedimentary logs (1:40) were augmented with 3D-photogrammetry (for methods, see Sørensen & Dueholm 2018) to reconstruct the relative position of fragmented outcrops and resolve stratigraphic problems (e.g. the thickness of the Bastians Dal Formation: see Fig. 3). Coal samples were collected for total carbon (TC), total sulphur (TS), total organic carbon (TOC), Rock-Eval-type pyrolysis, reflected light microscopy and vitrinite reflectance (VR). Sandstone samples, which displayed apparent staining, were also collected for TOC, Rock-Eval-type pyrolysis and reflected light microscopy. The methodologies used are summarised here. For full details, see Bojesen-Koefoed *et al*. (2020).

TC and TS were determined by combustion using a LECO CS-200 induction furnace. TOC was determined similarly after elimination of mineral-bound carbon by hydrochloric acid treatment, and recalculation based on loss of weight.

Rock-Eval-type screening pyrolysis was done using a HAWK (Wildcat Instruments, Humble, TX, USA) calibrated using the IFP160000 pyrolysis standard, ensuring comparability with standard Rock-Eval data. An in-house standard (Marl Slate, Sunderland Quarry, UK) was used for stability control. Parameters measured include S1 (hydrocarbons present in the sample mg/g), S2 (pyrolytic hydrocarbons, mg/g), S3 (pyrolytic CO_2, mg/g) and Tmax (temperature of maximum rate of pyrolytic hydrocarbon generation, °C) and the calculated parameters hydrogen index (HI; 100*S2/TOC), oxygen index (OI; 100*S3/TOC) and production index (PI; S1/(S1+S2)). For details of the Rock-Eval-type pyrolysis technique and its applications, see Espitalié *et al*. (1985) and Bordenave *et al*. (1993).

Preparations for reflected light microscopy were made according to standard procedures (Taylor *et al*. 1998) but modified to compensate for variations in settling velocity of particles of different density. The samples were crushed and sieved between 63 µm and 1 mm, and this fraction was embedded in epoxy. Blocks were subsequently cut vertically and remounted in epoxy with the cut surface upwards. The mounts were ground and polished to obtain a smooth surface for microscopy.

VR (random, oil immersion) was measured using a Leica DM4000M reflected light microscope (50 × objective and the Diskus Fossil system of Hilgers Technisches Buero for recording of measurements). Measurements were made at 546 nm (monochromatic light), with the microscope being calibrated against the YAG 0.903%Ro standard with integrated optical zero. The average VR for each sample was calculated from a population selected from the total reflectance histogram (= %Ro). In addition, samples were inspected in reflected white light and fluorescence-inducing blue light using a Zeiss microscope.

Results

Bastians Dal Formation

The Bastians Dal Formation overlies crystalline basement and is exposed in a series of broken outcrops, which can be traced over several kilometres along an N–S-aligned valley (Fig. 3), just beyond the headwaters of Bastians Dal itself. Eight sections were logged in detail (i–viii in Figs 3 and 4) through the Bastians Dal Formation. These logs provide the basis of the facies analysis presented here. The facies comprising the Bastians Dal Formation were briefly outlined by Alsgaard *et al*. (2003), who also formally defined the unit. Five facies are recognised in the present study: large-scale cross-bedded conglomerates, trough cross-bedded conglomerates, cross-bedded sandstones, fine-grained and rooted sandstones and siltstones and thin coals. The latter likely reflect the onset of conditions, which culminated in the deposition of the thicker coals, which define the overlying Muslingebjerg Formation.

Facies: large-scale cross-bedded conglomerates

This facies is characterised by large-scale planar cross-sets, which form beds up to 1.7 m thick. Bed bases are commonly mildly erosive, and relief is often noted across the unit tops. Cosets of cross-beds define amalgamated sediment bodies up to 3 m thick and 30 m wide, which contain low-angle internal truncation surfaces (Fig. 5A). Clasts are dominated by quartz-rich lithologies, range from sub-rounded to rounded and reach a maximum clast size of 30 cm, although

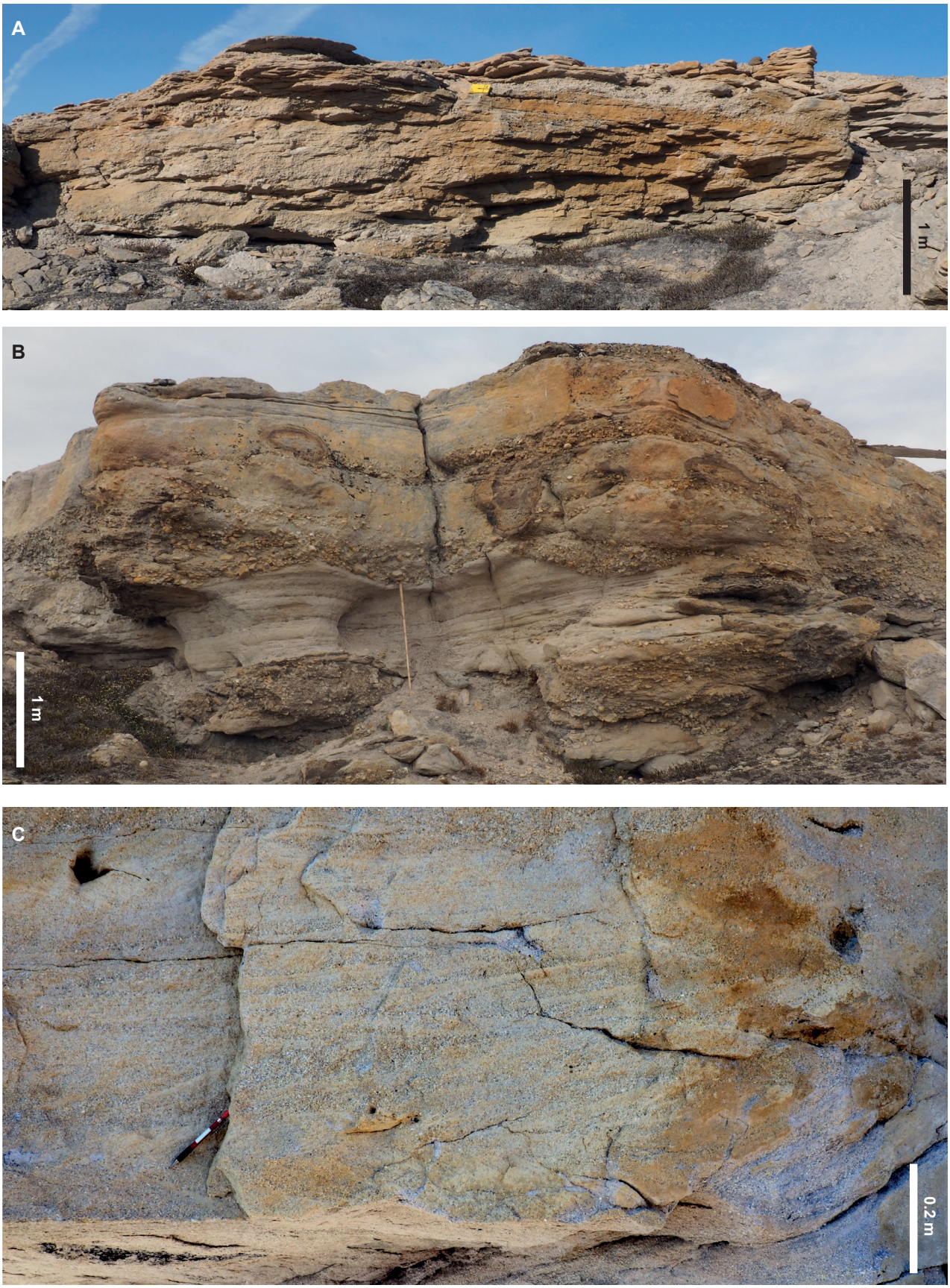

Fig. 5 Photographs illustrating the facies of the Bastians Dal Formation. **(A)** Large-scale cross-bedded conglomerates displaying low-angle truncation surfaces and bar-top relief (*c*. 69 m, Fig. 4). **(B)** Trough cross-bedded conglomerates with sharply erosive bases mantled with pebble (*c*. 115 m, Fig. 4). **(C)** Cross-bedded sandstones. Clear alternations of coarser-and finer-grained foresets can be observed, as well as voids, where coalified wood was once present (*c*. 103.5 m, Fig. 4) .

a maximum clast size of 10 cm is more common within individual beds. Coarser material is often concentrated towards the cross-set toes and some normal grading is recognised within individual laminae. Pebble-grade clasts are dominant and largely form supported conglomerates. Minor very coarse sand to granule material is recorded in some cross-laminae. Towards unit tops, tabular-bedded pebbly conglomerates displaying poorly defined horizontal lamination, minor imbrication and occasionally containing large coalified wood fragments (1.5 m long) are also recognised.

Palaeocurrents measured from both the planar cross-bedding and imbrication within this facies display a strong unidirectional palaeoflow to the SW (Fig. 6), which is consistent with the findings of Alsgaard *et al*. (2003).

Interpretation. The coarse-grained nature of this facies reflects deposition in a very high-energy environment. The strongly unidirectional flow, alongside the large-scale cross-bedding and amalgamated nature of the sediment units, suggests deposition as mid-channel bars within a coarse-grained fluvial system (Miall 1996). This is consistent with the preserved relief recognised at some unit tops (Fig. 5A). Individual cross-sets may reflect periods of increased flow within the system, particularly where grading is recognised. More tabular beds towards unit tops record bar-top processes, in some instances providing strand surfaces for woody debris that was washed downstream.

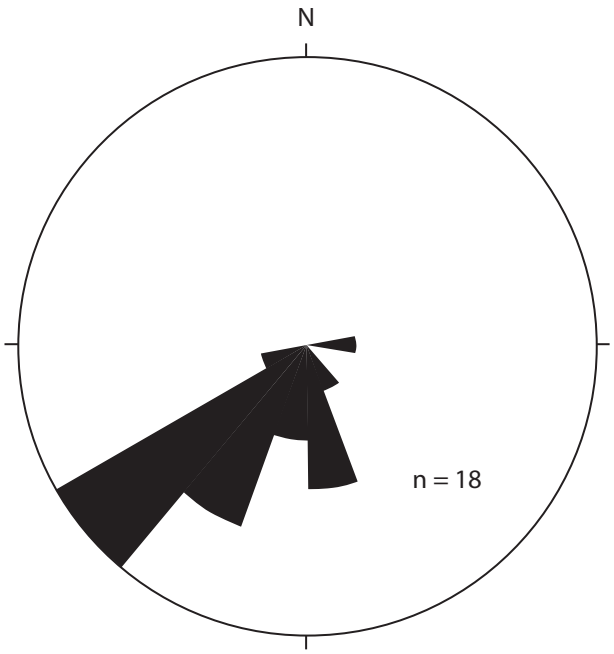

Fig. 6 Compiled trough cross-bedding, planar cross-bedding and imbrication palaeocurrent data from the Bastians Dal Formation (*n* = 18). Data were collected from thorughout the outcrop area.

Facies: trough cross-bedded conglomerates

The trough cross-bedded conglomerates contain troughs ranging from 0.2 to 0.5 m deep, which stack to form units up to 1.75 m thick. Troughs commonly have erosive bases mantled by coarser pebble lags and show a broad fining-up signature (Fig. 5B). Clasts up to 30 cm are found in the trough bases but pebble-grade material predominates, often fining-upwards to very coarse sand. Clast lithologies are dominantly quartz rich, and rounding ranges from sub-rounded to rounded. Imbrication is noted in places, and along with the trough alignment, provide evidence for SW-directed flow. Coalified wood fragments are recognised, often concentrated towards the unit tops where the grain size fines towards very coarse sand.

Interpretation. Trough cross-bedding is indicative of migrating sinuous-crested, linked dune forms. These are characteristic of sustained flow within channels and therefore are interpreted to reflect deposition where flow was focused between the mid-channel bars defined by the large-scale cross-bedded conglomerates. The fining-upward signature, often noted in individual troughs, suggests a flashy flow. It was probably during these flash-flood events that the wood fragments were washed into the system before being deposited during waning flow.

Facies: cross-bedded sandstones

Cross-bedded sandstones often appear to cap the coarser facies and, furthermore, appear to become more common up-section (Fig. 4). Planar cross-bedding predominates, forming sets ranging from 0.1 to 0.3 m thick and amalgamated beds up to 1 m thick. The cross-bedding is disrupted to form convolute lamination in places. Minor erosion is recognised at bed bases, in some instances defined by pebble lags and coalified wood fragments. Coalified wood fragments and associated voids are common throughout this facies. Grain size largely varies between very coarse to granule. Alternations in these grain sizes can be recognised between individual foresets (Fig. 5C), and some laminae display fining-up signatures. Compositioanlly the sediments are quartz dominated, but mica booklets up to 4 mm are also observed. This facies includes subordinate horizontally laminated sandstones and structureless sandstones. Both have a similar texture and contain 'floating' coalfield fragments.

Interpretation. This facies reflects deposition in much reduced energy conditions, in comparison with the conglomeratic facies. The predominance of planar cross-bedding indicates downstream migration of straight-crested dunes. The limited bed thickness and the association with horizontal lamination (high stage

flow) suggest deposition in relatively shallow water. Fluctuations in flow intensity, and therefore evidence for flashy flow, are indicated by the alternations in coarser and finer grain sizes between foresets. The fact that this facies caps the coarser-grained facies described earlier suggests deposition within areas of the fluvial system where channels are moving towards abandonment, as well as overbank areas. Where this facies begins to dominate the succession in the upper portion of the Bastians Dal Formation, it forms units up to 4.5 m thick. This appears to indicate a transition to lower-energy conditions related to the infilling of topography and the related denudation of the catchment regions. However, basement must still have been exposed locally to source intact mica booklets. Where these finer-grained intervals become more dominant in the upper portions of the succession, they are interpreted to record deposition in mobile, high width-to-depth ratio channels.

Facies: Fine-grained and rooted sandstones and siltstones

Between the coarser-grained facies, much of the Bastians Dal Formation is poorly exposed (Fig. 4). In some instances, fine-grained facies are preserved adjacent to the coarser units, and it is suggested that these likely reflect much of what comprises the poorly exposed sections. The sandstones in these exposures are fine to medium grained and form thin beds up to 0.3 m thick. Mica and coal fragments are common throughout these sandstones, in which current rippling and small-scale cross-bedding predominate. Rooting of bed tops is also common, and in some instances these surfaces are topped by thin (up to 0.2 m) bright, black to blue coals. These thin coals occur in the upper portion of the Bastians Dal Formation and likely herald a transition to the thick coals of the Muslingebjerg Formation. Intercallations of black, papery carbonaceous siltstones up to 0.3 m thick are also noted.

Interpretation. This facies reflects the lowest energy of deposition recorded in the Bastians Dal Formation. The presence of thin coals and rooted horizons provide evidence for *in situ* vegetation, leading to the development of organic-rich soils or peats. The presence of thin sands containing current ripples and small-scale cross-bedding likely record overbank flow and related crevasse splay deposition. Likewise, the papery siltstones probably reflect inundation of the overbank regions and the subsequent settling out of fines in standing bodies of water. These deposits are typical of overbank facies.

Stratal geometries and structural implications

The Bastians Dal Formation forms a series of broken outcrops that can be traced from the basement to the overlying Muslingebjerg Formation. Eight sections were logged in detail, and the thickness of the intervening non-exposed sections was calculated using photogeology. The coarse-grained elements can be traced across the outcrop area as prominent escarpments for over 500 m (Fig. 3A). A maximum thickness of 140 m was calculated for the Bastians Dal Formation, but mapping demonstrated thinning to both the north and the south (Fig. 2B), confirming previous suggestions that these deposits infill a palaeovalley. A predominantly south-westward palaeocurrent orientation was recorded throughout the succession (Fig. 6), which likely reflects the orientation of the palaeovalley. This alignment is consistent with faulting, which appears to control the thickness of the overlying Muslingebjerg Formation (described next). Thus, faulting may also have exerted a control on the orientation of the palaeovalley when the fluvial deposits of the Bastians Dal Formation were deposited. The fining-upward signature recorded by the occurrence of fine-grained and rooted sandstones and siltstones in the upper part of the formation is consistent with an infilling of topography and the related denudation of the catchment regions.

Muslingebjerg formation

The base of the Muslingbjerg Formation is not visible where the unit is formally defined on Hochstetter Forland (Surlyk 1977; Surlyk *et al*. 2021). From what is seen in Bastians Dal, it appears that the basal part of the formation interfingers with fluvial deposits of the Bastians Dal Formation. However, as Surlyk (1977) and Surlyk *et al*. (2021) consider the Muslingebjerg Formation to be characterised by thick coal seams, we regard the base of this unit to lie below the first significant coal seam encountered (1.5 m thick). The upper boundary is placed at the base of the continuous marine sandstones of the Pelion Formation. In this study, two sections through the Muslingebjerg Formation were logged in detail: Bastians Dal north (Fig. 7; referred to as the 'northern section'), where the coals are interbedded with fluvial facies similar to those of the Bastians Dal Formation, and Bastians Dal south (Fig. 8; referred to as the 'southern section'), where coals are interbedded with the facies described below.

Three facies dominate in the Muslingebjerg Formation in the southern section: low-angle cross-bedded sandstones, planar cross-bedded sandstones (with or without bundling) and coal. A single occurrence of trough cross-bedded sandstones is also recorded, and this appears to have closer affinities to the facies found in the Bastians Dal Formation. In the north of the study region, cross-bedded sandstones similar to the underlying Bastians Dal Formation are recorded within the Muslingebjerg Formation.

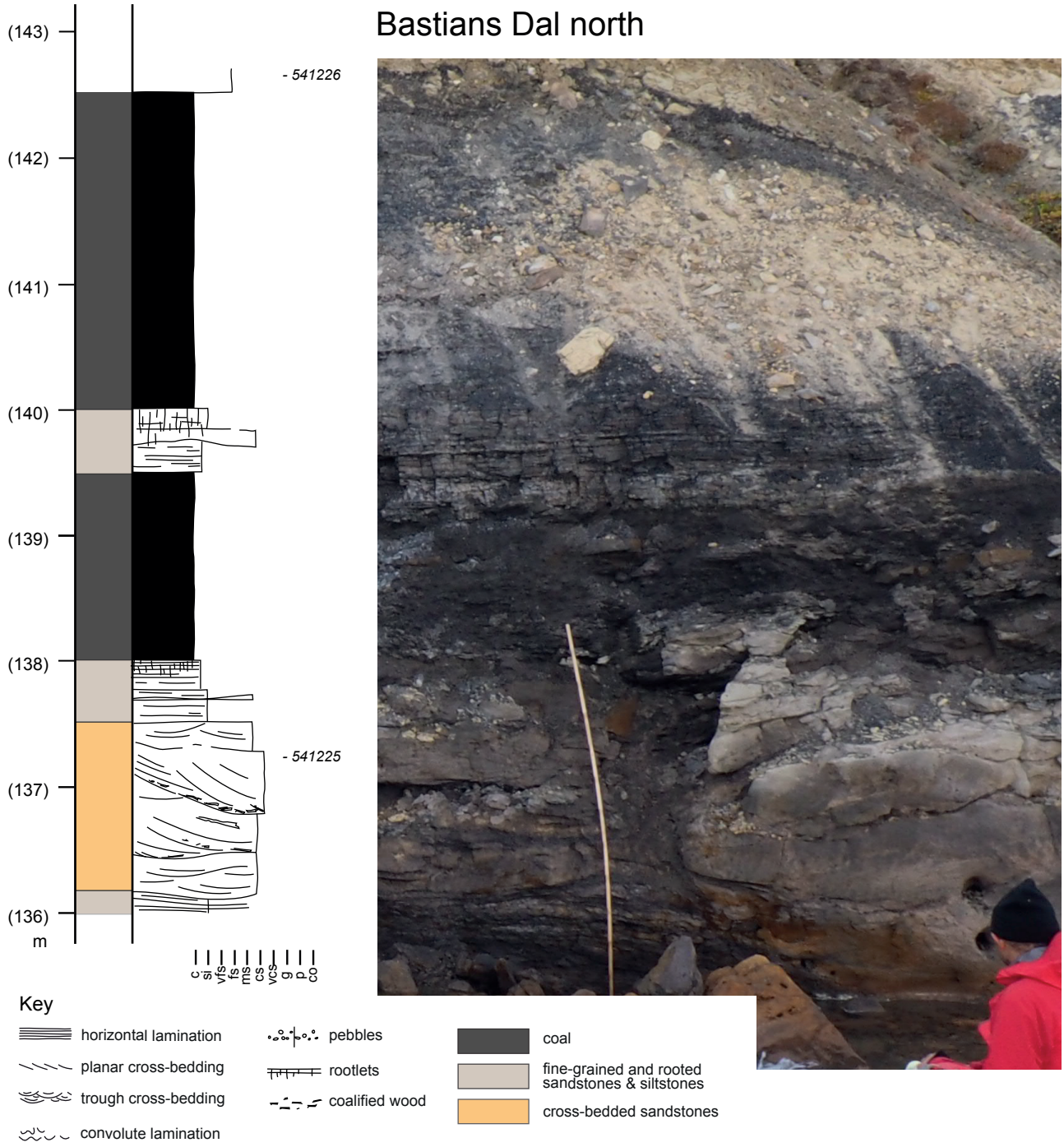

Fig. 7 Sedimentological log and accompanying photograph of the thickest coal found in the Muslingebjerg Formation (**ix** in Fig. 3A). This exposure is found in northern Bastians Dal. Much thinner than its southern counterpart, the associated facies have a greater affinity to the underlying Bastians Dal Formation. Location in Fig. 2. Samples collected from this section are numbered to the right of the log.

Facies: low-angle cross-bedded sandstones

The low-angle cross-bedded sandstones form beds up to 2.8 m thick and are characterised by cross-bedding dipping 8–10° to the southwest (Fig. 9A). Bundling of the cross-laminae is noted within the low-angle cross-bedding, forming laminae bundles 0.1–0.2 m thick. These are sometimes highlighted by the presence of more intensely cemented intervals. Small-scale cross-bed sets, 0.15 m thick, are also enclosed within the low-angle cross-sets. Well-developed wave ripples are also recorded (Fig. 9C). The fine-sand grain size is largely uniform throughout this facies, although some pebble-grade coal fragments are present at some bed bases. Only minor bioturbation is recorded in the logged sections but latterally, better defined *skolithos* and *thalassinoides* are noted alongside bivalve casts (Fig. 9B).

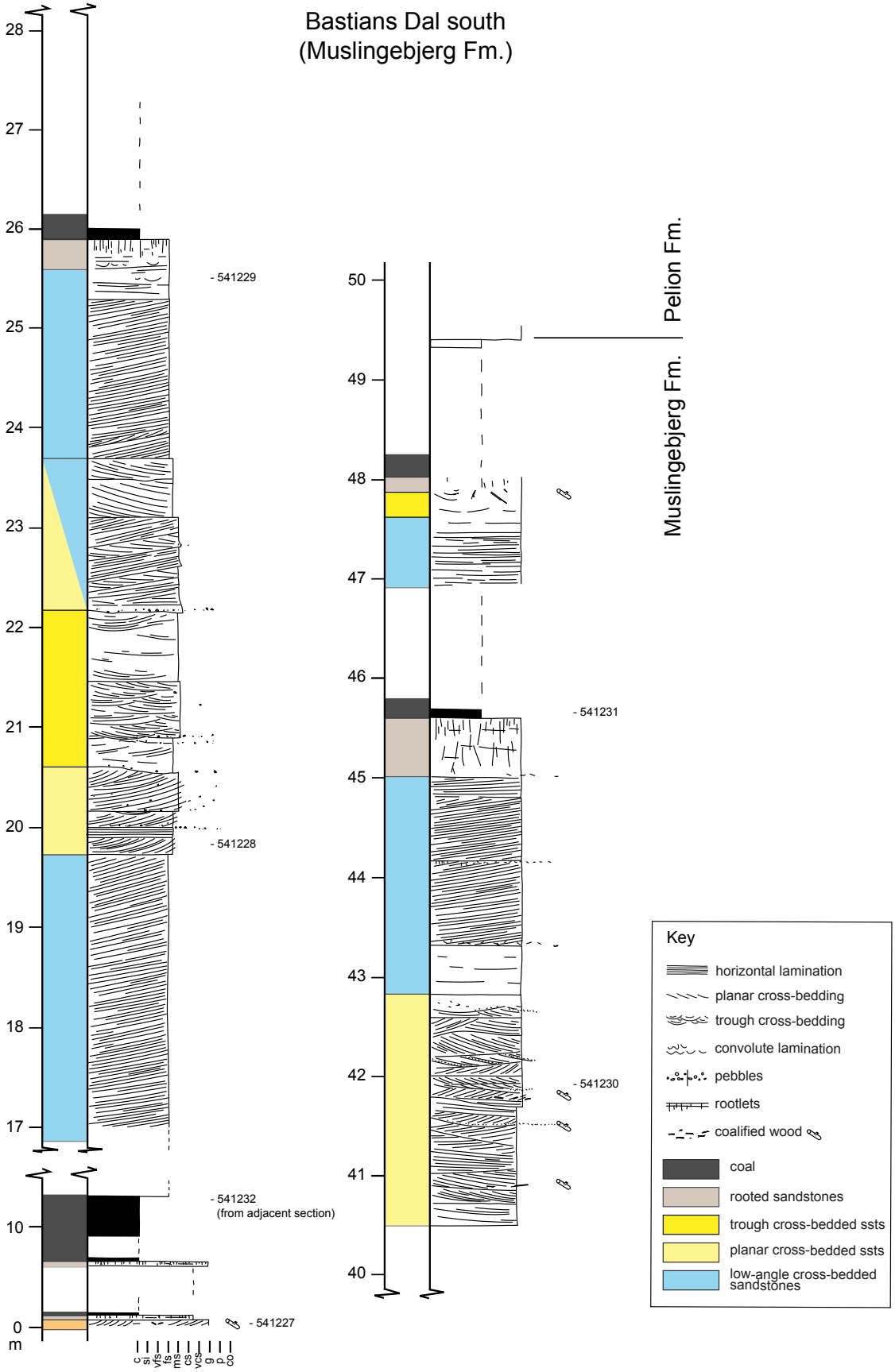

Fig. 8 Sedimentological log through the Muslingebjerg Formation in southern Bastians Dal. Here, the succession is greatly expanded by the occurrence of shallow-marine sandstones. Location and position of the log in Figs 2 and 3B. Samples collected from these sections are numbered to the right of the logs.

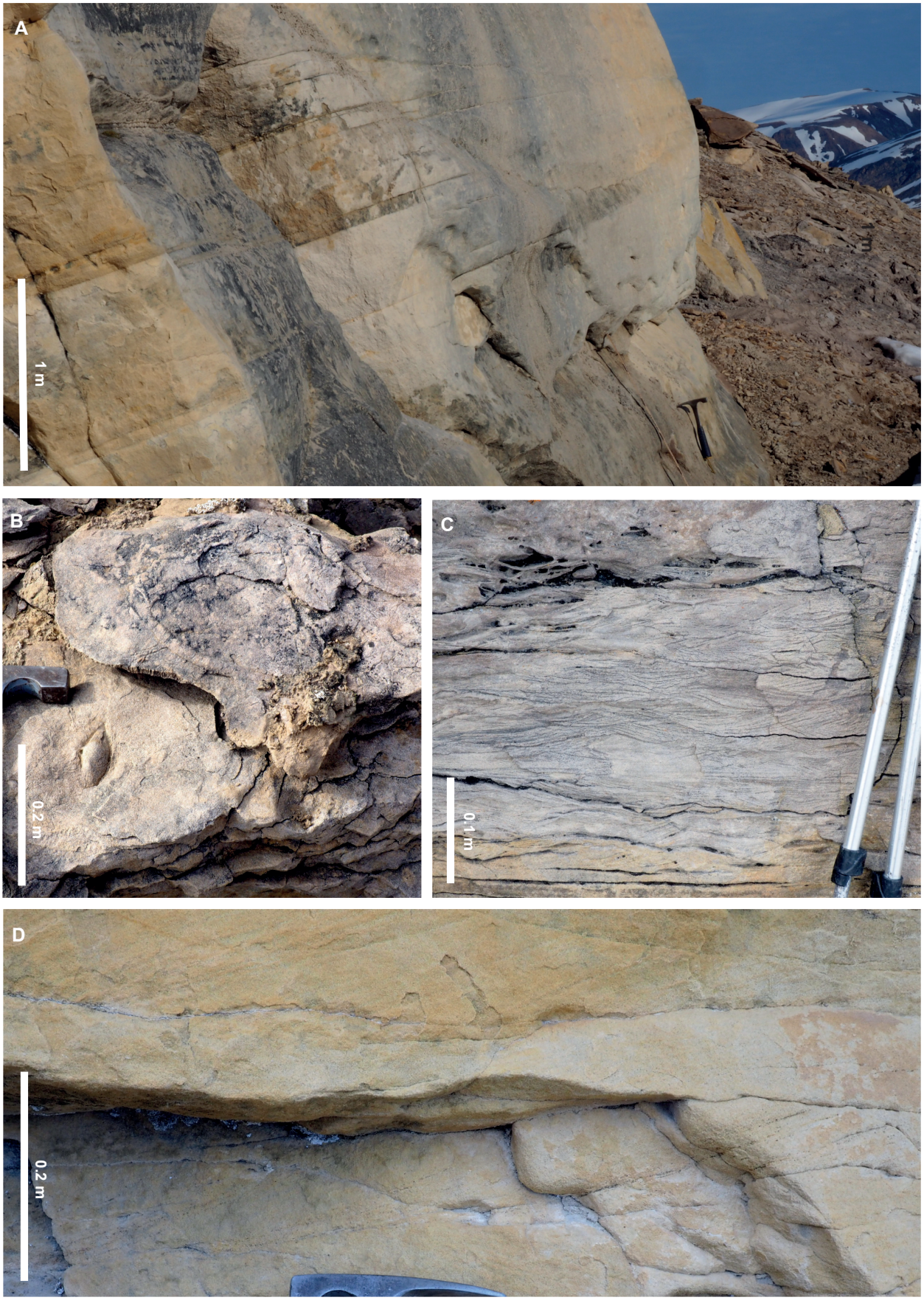

Fig. 9 Photographs illustrating the facies of the Muslingebjerg Formation. **(A)** Low-angle cross-bedded sandstones (*c*. 18 m, Fig. 8). Cross-bedding truncated by a horizontal erosion surface towards the top of the section. **(B)** Bivalve moulds and bioturbation within the low-angle cross-bedded sandstones. **(C)** Wave rippling associated with the low-angle cross-bedded sandstones. **(D)** Planar cross-bedded sandstones. Bundled foresets are distinctly visible in the lower bed where the bundling is highlighted by coalified wood fragments (*c*. 21 m, Fig. 8).

Interpretation. Large-scale low-angle cross-bedding is typical of upper shoreface environments (e.g. Ahokas *et al*. 2014), where it is developed through swash and backwash processes. The assemblage of bioturbation and bivalve casts suggest shoreface development in a marine environment. Apparent bundling of foresets may reflect a tidal influence, but could also result from varying energy conditions within the shore zone. Small-scale cross-bedding within the larger cross-sets, and the prescence of wave rippling, records the migration of smaller scale bedforms across the shoreface and probably reflects the transition to slightly deeper water. The concentration of coal fragments at bed bases can be interpreted as recording periods of shore-zone reorganisation resulting from low-frequency, high-magnitude storm events. These events will have resulted in erosion of back-beach areas and the liberation of organic material. They may have also generated hummocky cross-stratification in the lower shoreface and offshore transition zone, which would have lain offshore to the south-east.

Facies: planar cross-bedded sandstones (with or without bundling)

This facies comprises fine- to medium-grained sandstones displaying planar cross-bedding in beds up to 0.4 m thick. In some examples, the cross-bedding displays well-developed bundling, defined by alternating foresets of coarser and finer grain sizes, as well as variation in the thickness of these couplets. A cyclic inclusion of coaly fragments also occurs in some instances (Fig. 9D). Regular truncations are noted within the cross-bedding, and the basal portions of the cross-sets often contain concentrations of granule to small pebble-grade material. Coalified wood fragments are also common along bed bases. Minor trough cross-bedding and horizontal lamination are also observed within this facies.

Interpretation. The well-developed bundling within the planar cross-bedded sandstones is characteristic of tidal processes. Deposition under the influence of tidal currents is recorded by the observed variation in grain size in the forsets, and the bundling of foreset couplets, which reflect longer-term variations (neap-spring) in tidal range. Therefore, this facies is interpreted as the deposits of tidal dune fields. Occurences of coarser grain sizes and regular inclusion of coalified material suggest a greater link to the fluvial input recorded in the northern section. This is also consistent with the relationship between this facies and the trough cross-bedded sandstones described next.

Facies: trough cross-bedded sandstones

Trough cross-bedded sandstones are found as a single interval, *c*. 1.3 m thick, in the upper sandstone unit of the southern section of the Muslingebjerg Formation (Fig. 8). The sandstones are medium grained and the cross-beds are up to 0.6 m thick, but set thicknesses of 0.1–0.2 m dominate. Granules and small pebbles are concentrated along erosive bed bases.

Interpretation. The facies appears to display affinities with the fluvial deposits of the Bastians Dal Formation. The erosional bed bases and dominance of trough cross-bedding, the latter indicative of sustained flow, along with the absence of marine indicators, favours a similar depositional setting. Therefore, the trough cross-bedded sandstones are interpreted as fluvial-channel deposits. This demonstrates that the fluvial system recorded in the facies of the northern section intermittently reached southwards, likely as a result of fluctuations in sea level.

Facies: coals

The coals are best exposed in the northern section where 1.5 and 2.5 m thick coal beds are separated by a thin interval of sandstone (Fig. 7). Coal beds in the south of the study area, although poorly exposed, appear to reach up to 5 m in thickness. The coals themselves are brittle to friable and bright black to blue. Some portions contain alternations of more silty material. The base of the coals is often marked by well-developed root networks, which penetrate underlying sandstones to a depth of up to 0.6 m. In the southern section, an oily slick was observed on water issuing from below one of the coal beds.

Interpretation. The precursor peats of the coals are interpreted as representing deposition in swampy environments on the fluvial plain (northern section) or coastal plain (southern section). The commonly rooted nature of the underlying sandstones demonstrates autochonous peat formation. The relatively thick coals indicate damming of groundwater, perhaps due to base-level rise caused by a rise in relative sea level. These processes may have resulted in waterlogged, sediment-starved conditions favourable for peat accumulation and preservation. In Hochstetter Forland, *c*. 40–50 km north of Kuhn Ø (Fig. 2), liptinite-rich coals of the Muslingebjerg Formation are present. These have a very good to excellent potential for petroleum generation, which has been interpreted to be governed by marine influence in a coastal-mire depositional setting (Bojesen-Koefoed *et al*. 1996; Petersen & Vosgerau 1999; Petersen *et al.* 1998). The interbedding of shallow-marine sediments with coals in the southern section suggests a similar depositional setting as on Hochstetter Forland. The coals of the northern sections, which are interbedded with fluvial deposits, were analysed for their source rock potential by Petersen *et al*. (2002) who characterised them as humic coals that

Table 1 Results of coal and bitumen analysis.

Lithology	Sample number	TOC	TC	TS	Tmax	S1	S2	S3	HI	OI	PI	Ro	n	STD
		(wt%)	(wt%)	(wt%)	(°C)	(mg HC/g)	(mg HC/g)	(mg CO_2/g)				(%)		
Sandstone	541228	0.26	0.17	0.04	416	0.00	0.06	0.42	23	162	0.00			
Sandstone	541229	0.48	0.63	0.06	426	0.02	0.11	0.70	23	146	0.15			
Coal	541231	51.47	55.99	4.88	418	0.98	51.65	30.46	100	59	0.02	0.36	100	0.025
Coal	541232	45.64	49.40	2.45	424	0.73	76.43	10.79	167	24	0.01	0.40	100	0.039
Coal	541235	47.65	52.91	3.64	418	0.70	33.89	31.95	71	67	0.02	0.39	100	0.026

TOC: total organic carbon (wt%). TC: total carbon (wt%). TS: total sulphur (wt%). Tmax: from Rock-Eval-type pyrolysis, temperature of maximum pyrolysate-yield (°C). S1, S2, S3: parameters from Rock-Eval-type pyrolysis. HI: hydrogen index, 100 × S2/TOC. OI: oxygen index, 100 × S3/TOC. PI: production index, S1/(S1 + S2). Ro: vitrinite reflectance (%), random mean in oil. n: number of particles measured and used. STD: standard deviation of Ro population. Sample locations in Fig. 8.

represent only a marginal source-rock type. However, the observation of an oily slick on water originating from the base of one of the coal beds raises the possibility that some of these coals may also have a potential for petroleum generation. The following analysis provides a more detailed investigation of these relationships.

Coal and bitumen analysis

Three coal samples were analysed: one from the lower seam (541232) and two from the upper seam (541231 and 541235) – all from the southern exposures of the Muslingebjerg Formation (results in Table 1; locations in Fig. 8). All coal samples are thermally immature, showing VR values in the range of 0.36–0.40 %Ro and corresponding Tmax in the range of 418–424°C.

The coals are relatively rich in mineral matter, shown by TOC in the range of 45–52 wt%, and based on the difference between TC and TOC, significant proportion of the mineral content is carbonate. Sulphur contents are rather high (2–5 wt%).

The petroleum generation potential of the coal samples is within the range of other samples that have been analysed from the same location (Figs 10A, B). All three samples are initially classified as predominantly gas-prone, but sample 541232 differs in showing higher HI and lower OI (Table 1). Using the method of Dahl *et al*. (2004) to assess the properties of the live kerogen fraction, a regression line has been constructed for the 'Lower Seam' of Petersen *et al*. (2002; Fig. 10C which demonstrates that this seam indeed has a high proportion of 'dead carbon' (25.5%) and that the live kerogen fraction is clearly oil-prone (Fig. 10C). Sample 541232 falls exactly on this regression line.

Microscopic inspection of sample 541232 shows a composition dominated by huminite-group macerals, particularly eu-ulminite, but with a fair proportion of resinite present. Other liptinite-group macerals are sparsely present (Figs 11A, B). Fractures within huminite particles frequently show dark discolouration along their margins as well as associated refraction phenomena akin to the well-known 'Newton's rings', caused by liquid bitumen filling the fractures (Figs 11C, D).

Two sandstone samples (samples 541228 and 541229) were collected adjacent to the coals (results in Table 1; locations in Fig. 8). They were suspected of being stained by petroleum, and each yield different results. Sample 541228 shows low TOC (0.26 wt%), very low pyrolysis yield (S2 = 0.06 mg/g) and a PI of zero. Sample 541229 shows somewhat higher TOC (0.48 wt%) and a low pyrolysis yield (S2= 0.11 mg/g), but a PI of 0.15, which may suggest light staining. However, the absolute values of S1 and S2 used in the calculation of PI are very small and thus call for caution (Fig. 10D). The difference between TC and TOC indicates the presence of carbonate.

Microscopic examination of sample 541229 reveals small patches of bitumen along pores and in pore throats, and pores lined with a thin carbonate cement (Figs 12A, C). Bitumen shows a dull, brownish fluorescence, whereas the carbonate cement appears yellow (Figs 12B, D).

Interpretation

The Muslingebjerg Formation in Bastians Dal represents the transgression of an infilling palaeovalley. Hence, coals in the southern outcrops and the lower part of the succession may be more prone to marine influence (resinite enriched) than coals which formed updip, and higher in the succession (humic), and thus show higher petroleum potential (Petersen *et al*. 1998). Elements of marine influence are also hinted at by the slightly higher than expected levels of sulphur observed, reflecting the relatively sulphate-enriched character of marine water. Thermal maturity is low, and clearly below the threshold for petroleum generation. However, the presence of bitumen-filled fractures in sample 541232 (lower seam) is still not surprising, since some resinite is known to generate liquid petroleum at a very early stage in the maturation process (e.g. Snowdon & Powell 1982; Khorasani & Murchison 1988; Snowdon 1991).

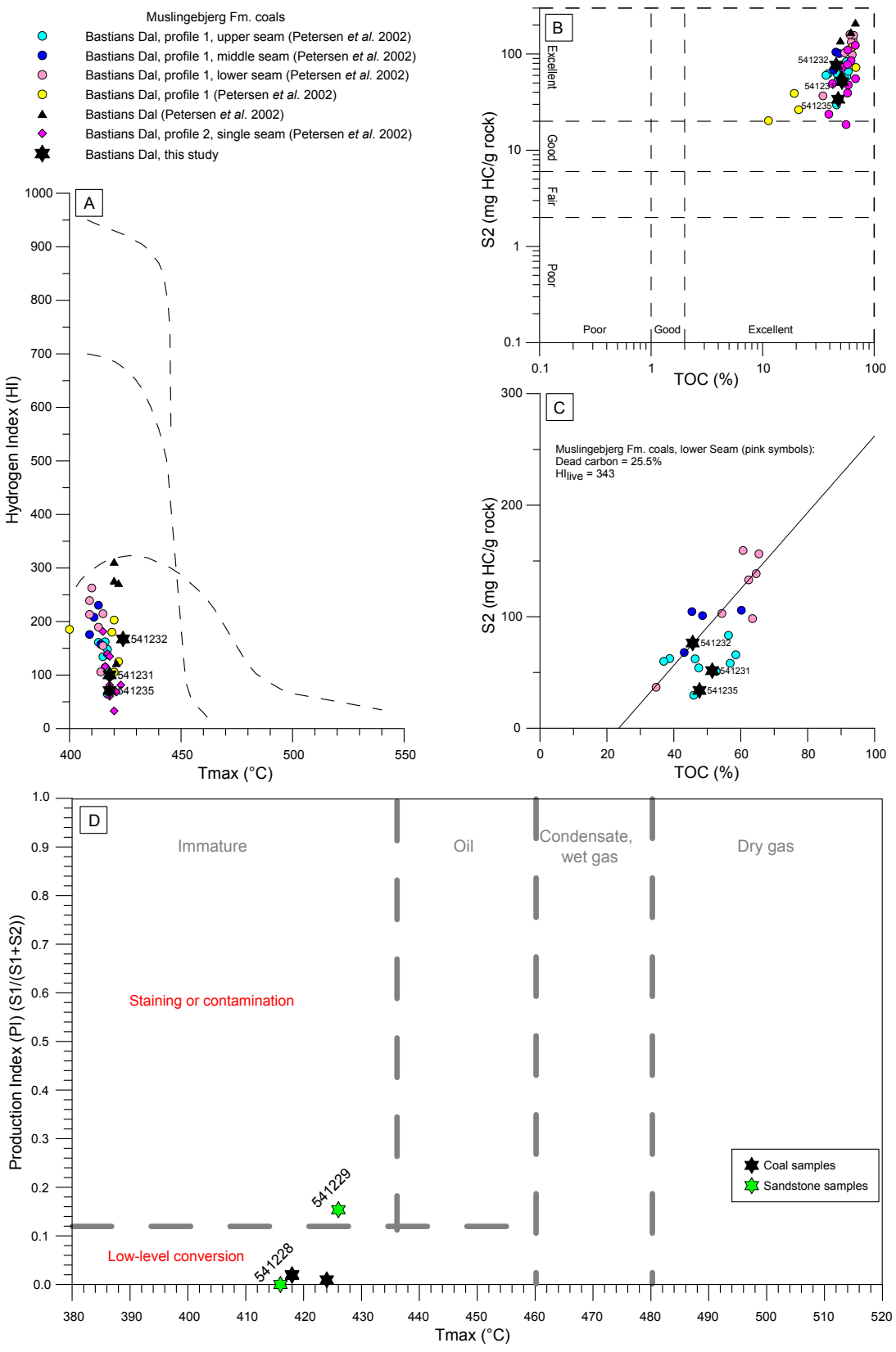

Fig. 10 Rock-Eval-type screening pyrolysis data for samples from Bastians Dal. For comparison, data from the present study are plotted together with data on coal samples from the same location, published by Petersen *et al*. (2002). **(A)** Standard-plot of Tmax vs. hydrogen index (HI). Samples from the present study all fall within the range of previously published samples. Sample 541232 shows somewhat higher petroleum potential than samples 541231 and 541235. **(B)** Standard-plot of TOC vs. S2. Samples from the present study all fall within the range of previously published samples. **(C)** Linear plot of TOC vs. S2. Following the method of Dahl *et al*. (2004), a regression line has been constructed for the lower, more prolific seam, suggesting high levels of inert carbon, but also high petroleum potential of the live kerogen fraction (HI_{live}). Sample 541232 falls on the regression line. **(D)** Standard plot of Tmax vs. production index (PI). Only samples from the present study are shown. Sandstone sample 541229 appears lightly stained, whereas 541228 does not.

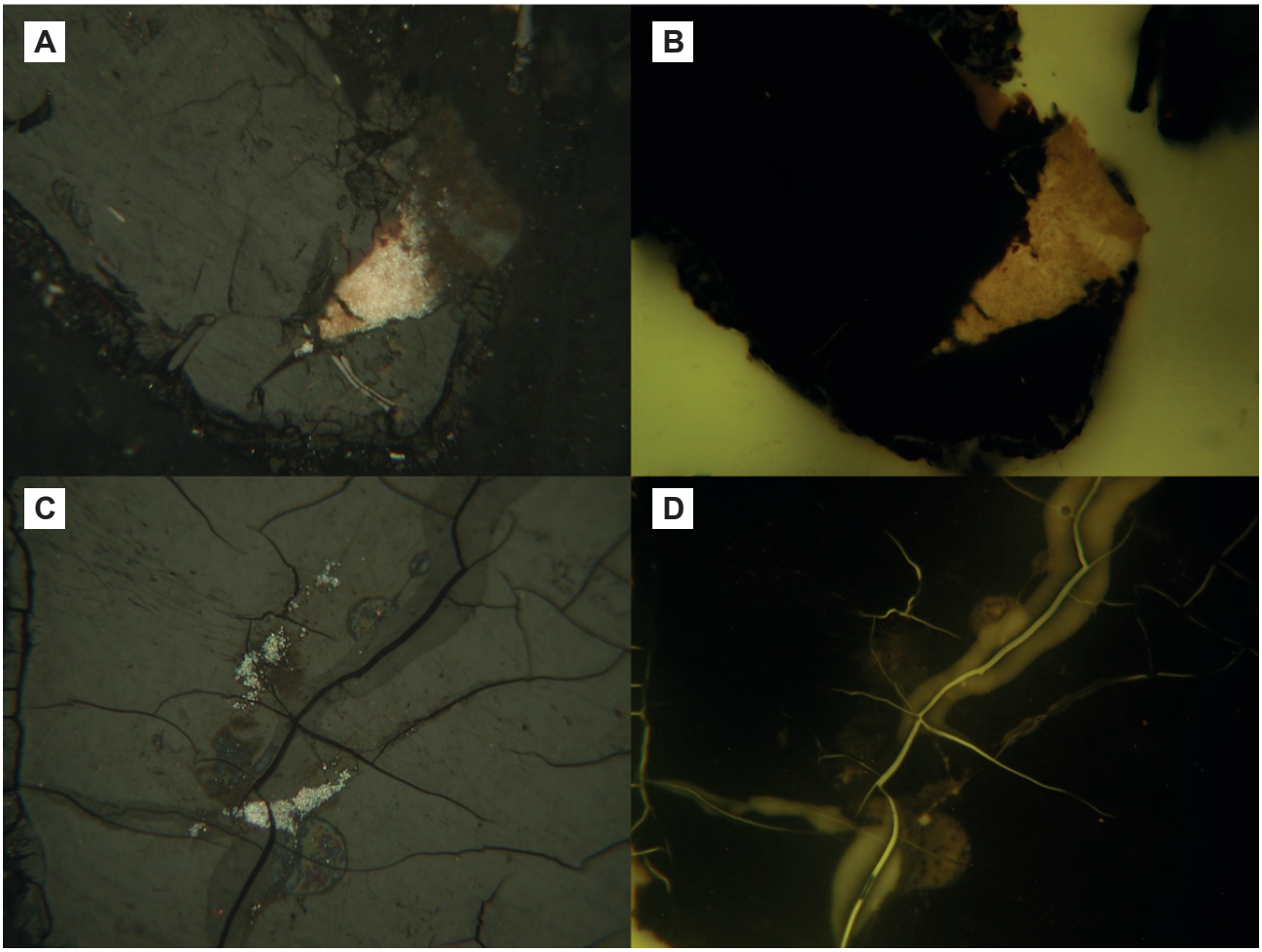

Fig. 11 Photomicrographs of coal sample 541232. Width of field approximately 300 µm. **(A)** Huminite particle (grey) enclosing lump of resinite (bright pinkish yellow). **(B)** Field as A. Fluorescence-inducing blue light. **(C)** Huminite particle with minute fractures showing discolouration along the rims due to liquid bitumen. Refraction anomalies akin to 'Newton's rings' are caused by bitumen from the fractures dissolving into the immersion oil used for microscopy. **(D)** Same field as C. Fluorescence-inducing blue light. Note the presence of fluorescence of the petroleum-stained rims of the fractures and blooming phenomena at refraction anomalies.

Petersen *et al*. (2002) note that in cases where the proportion of liptinite in coals from Bastians Dal exceeds a few per cent, the excess liptinite is resinite. Since resinite is the main liptinite-group maceral observed in sample 541232, we assume that the liquid bitumen observed represents products of early generation from resinite.

Highly oil-prone resinite-rich coals (Payer Dal, on Kuhn Ø and Hochstetter Forland, north of Kuhn Ø) are known from the Muslingebjerg Formation (Bojesen-Koefoed *et al.* 1996; Petersen *et al*. 1998, 2002). Such coals are even found as erratic blocks on the coasts of Norway (Horn 1931; Bojesen-Koefoed *et al.* 1996; Petersen *et al*. 2013). These coals are paralic, representing selective concentration of liptinite-group macerals, particularly resinite. Humic coals are also common in the Muslingebjerg Formation, such as those found in the northern outcrops visited in this study, and reported by Petersen *et al*. (2002), which are not conspicuously oil-prone (Petersen *et al*. 1998, 2002; Bojesen-Koefoed *et al.* 2012). The findings of the present study are in line with data published previously by Petersen *et al*. (2002). The close similarity between sample 541232 and samples of the 'Lower Seam' of Petersen *et al*. (2002) is striking.

Although the absolute values of S1 and S2 yielded by the sandstone sample 541229 are indeed low, the presence of light staining is confirmed by microscopy, with the dull fluorescence probably resulting from oxidation. Given the low level of thermal maturity of the succession in general, this result is somewhat surprising. Although generation of petroleum at low levels of thermal maturity is demonstrated by the coal sample 541232, expulsion of petroleum products, that is, secondary migration, requires prior saturation of the pores of the source rock. This will not take place unless the concentrations of resinite are much higher than those observed here. The presence of staining, even at the trace level observed here, could indicate that intervals with higher resinite concentrations are present somewhere in the succession, and that such intervals are able to expel small amounts of petroleum products even at

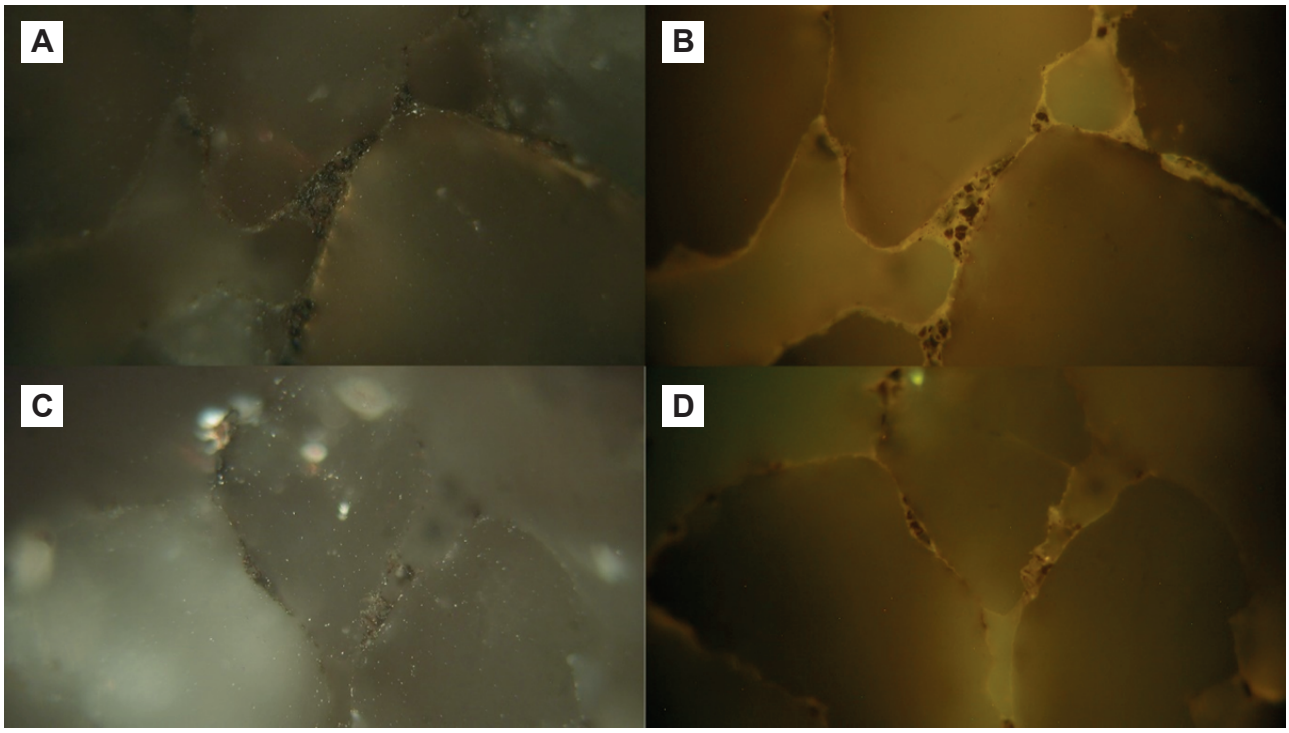

Fig. 12 Photomicrographs of sandstone sample 541229. Width of field approximately 300 µm. (**A** and **C)** Rounded quartz grains, pore surfaces lined with patchy, thin coatings of bitumen and carbonate cement. (**B)** Same field as A. Fluorescence-inducing blue light. (**D)** Same field as C. Fluorescence-inducing blue light. Pore-throats show accumulations of clay and dull brownish-fluorescing bitumen and other organic particles. Pores are lined by a thin carbonate cement (yellow fluorescence).

low levels of thermal maturity. At present, little evidence is available to substantiate this, although such prolific resinite-rich deposits are known from Payer Dal (Kuhn Ø) and Hochstetter Forland.

Stratal geometries and structural implications

The Muslingebjerg Formation thickens rapidly from north to south, across the exposures of central Kuhn Ø. In the north, the Muslingebjerg Formation is *c*. 5 m thick. Here it comprises two coal beds separated by 0.5 m of muddy siltstones and a thin coarse sandstone bed (Fig. 6), which closely resembles the facies of the underlying Bastians Dal Formation. In the south, a more complex and expanded (*c*. 50 m thick) succession is recorded (Fig. 8). This consists of three finer-grained and more poorly exposed units, divided by two thick sandstone successions. The finer-grained units appear to be dominated by coaly material, but the poor exposure does not allow more detail to be gained. The coals are best exposed immediately above the sandstone units, which often contain extensive rooting below the contact.

In the southern outcrops, the lowermost fine-grained interval (13 m thick) contains thin intercalations of coarse-grained sandstones, similar to the underlying Bastians Dal Fomation facies. As described earlier, it seems likely that peat accumulation was initiated due to a rising water table linked to a rise in relative sea level. A continued rise in relative sea level led to the transgression of the swampy, peat-forming environment, and eventually the depostion of a shallow marine succession, comprising shoreface and tidal dune-field elements, which display an overall coarsening-upward motif. Up-dip, in the northern outcrop region, fluvial deposition continued, and at times the fluvial influence can be recognised to extend southwards (trough cross-bedded sandstone facies). Coal, with associated rooting, caps the lower sandstone unit and likely reflects a basinward shift in facies, resulting from falling relative sea level. However, the continued accumulation of coal suggests elevated water tables and therefore a return to transgressive conditions. The capping of this second coal with a coarsening-upward package of shallow-marine sandstones suggests the eventual flooding of the peat-forming environment before relative sea level stabilised, as described from the lowermost coal-sandstone couplet. This pattern is repeated twice more, before being capped by the thick shallow-marine Pelion Formation.

The marked thickening in the Muslingebjerg Formation teminates abruptly against a NE–SW-aligned fault in the south of the study area (Fig. 2). This previously unknown structure defines the southward extent of the Muslingebjerg Formation, with only a much reduced thickness of the Bastians Dal Formation continuing south across the fault. The thick development of the Muslingebjerg Formation and its intercalation of marine

sandstones to the south reflect enhanced accommodation space available for deposition in this area. To the north, the Muslingebjerg formation is considerably thinner and the coals are intercalated with fluvial sediments. The variation in stratal thickness and facies was probably governed by syn-sedimentary subsidence along the fault, which limits the extent of the Muslingebjerg Formation to the south.

Placed into a wider regional sequence stratigraphic framework, in the broadest sense, the Muslingebjerg Formation can be viewed as part of a transgressive sequence tract (TST), where the boundary to the overlying Pelion Formation represents regional marine flooding. This of course can be broken down into considerably more detail. Petersen *et al.* (2002) considered each coal-sandstone couplet to represent a sequence, with the rooted surface found at the sandstone top defining the sequence boundary (reflecting a basinward shift in facies). In this interpretation, the coal formed during the TST and the sandstone formed during the highstand systems tract (HST). Even higher-order units were suggested by Petersen *et al*. (1998), where dulling-upward cycles were recognised within the coals. Coal analysis of comparable detail was not possible during this study. An alternative interpretation could be considered where the lowermost and poorly exposed section of the Muslingebjerg Formation in the southern outcrops would represent a TST, with the upper portion, including the two shallow-marine sandstone units, recording forestepping parasequences of the HST (e.g. Holz *et al*. 2002; Ketzer *et al*. 2003). If this were the case, the sandstone and coal couplets would be genetically linked to the overlying Pelion Formation.

Geological structure

Fault control on the distribution and thickness of the Muslingebjerg Formation provides evidence for the earliest stages of Jurassic rifting in the region. North of Kong Oscar Fjord (*c*. 72°N), the Early Jurassic is characterised by uplift and erosion. This is replaced by rift-related tilting of fault blocks and onlap of the pre-Jurassic basement from the Bathonian with rift climax reached during the latest Jurassic (Surlyk & Ineson 2003). Jurassic rifting in this region is largely characterised by N–S fault orientations (Surlyk 2003; Guarnieri *et al.* 2017). This is a distinct change from the NE–SW-oriented faulting that dominates the Triassic (Guarnieri *et al*. 2017; Andrews *et al*. 2021).

The Bastians Dal and Muslingebjerg Formations are constrained as no younger than the Middle Bathonian (see discussion in the Introduction section) and therefore provide an important insight into the nature of the earliest phases of rifting in the region. The earliest deposits, the Bastian Dal Formation, infill an NE–SW-aligned palaeovalley. This is oblique to the proposed N–S orientation of faulting related to rifting through the Mid to Late Jurassic (Surlyk 2003; Guarnieri *et al.* 2017). The exploitation of pre-existing basement weaknesses related to earlier phases of rifting could explain palaeovalley development on such an alignment. The discovery of an NE–SW-oriented fault in the south, into which the Muslingebjerg Formation thickens, confirms that active rifting on NE–SW-oriented faults occurred at this time. Post Pelion Formation, reverse movement also appears to have occurred before the fault became inactive, as evidenced by displacements on the Pelion Formation and the uninterrupted nature of the overlying Bernbjerg Formation (Fig. 3B). It seems likely that the alignment of the Bastians Dal palaeovalley was therefore, to some extent, also controlled by the fault activity recognised to control the thickness of the Muslingebjerg Formation. The NE–SW alignment of the palaeovalley and the faulting that controlled the distribution of the Muslingebjerg Formation are similar to pre-Jurassic and Triassic phases of rifting (Guarnieri *et al*. 2017; Andrews *et al*. 2021). Furthermore, faulting on this alignment can be traced SW to a fault, suggested to be of Triassic age (figs 2 and 9 in Guarnieri *et al*. 2017), which cuts Lindeman Fjord and follows the valleys east of the A. P. Olsen Land plateau, suggesting more than just a localised occurrence.

If the earliest phases of Middle Jurassic (Bathonian) rifting followed the structural trends established during the Triassic, it would suggest that it was during this period that a shift in stress fields occurred. Constraining the timing of this shift may help us elucidate the controls on these changes. This discovery further implies that the proposed Triassic structural grain is consistent northwards from Jameson Land (*c*. 70–72°N) where it was first recognised and therefore is likely to have also exerted a major control on facies distribution in more northern regions.

Synthesis

The Bastians Dal Formation (140 m) records the deposits of a high-energy gravel-bed river that flowed through an NE–SW-oriented palaeovalley (Fig. 13). Large-scale gravel bars were separated by channels, along which migrated sinuous-crested dunes. The outcrop available does not allow for the confident identification of the fluvial planform. Recent studies (e.g. Hartley *et al*. 2015; Swan *et al*. 2018) have demonstrated that great caution should be taken when attempting to identify planform from limited two-dimensional outcrops. Flow was likely flashy, and during flood events overbank areas accumulated straight-crested dunes and finer-grained deposits, some of which supported vegetation. Thin

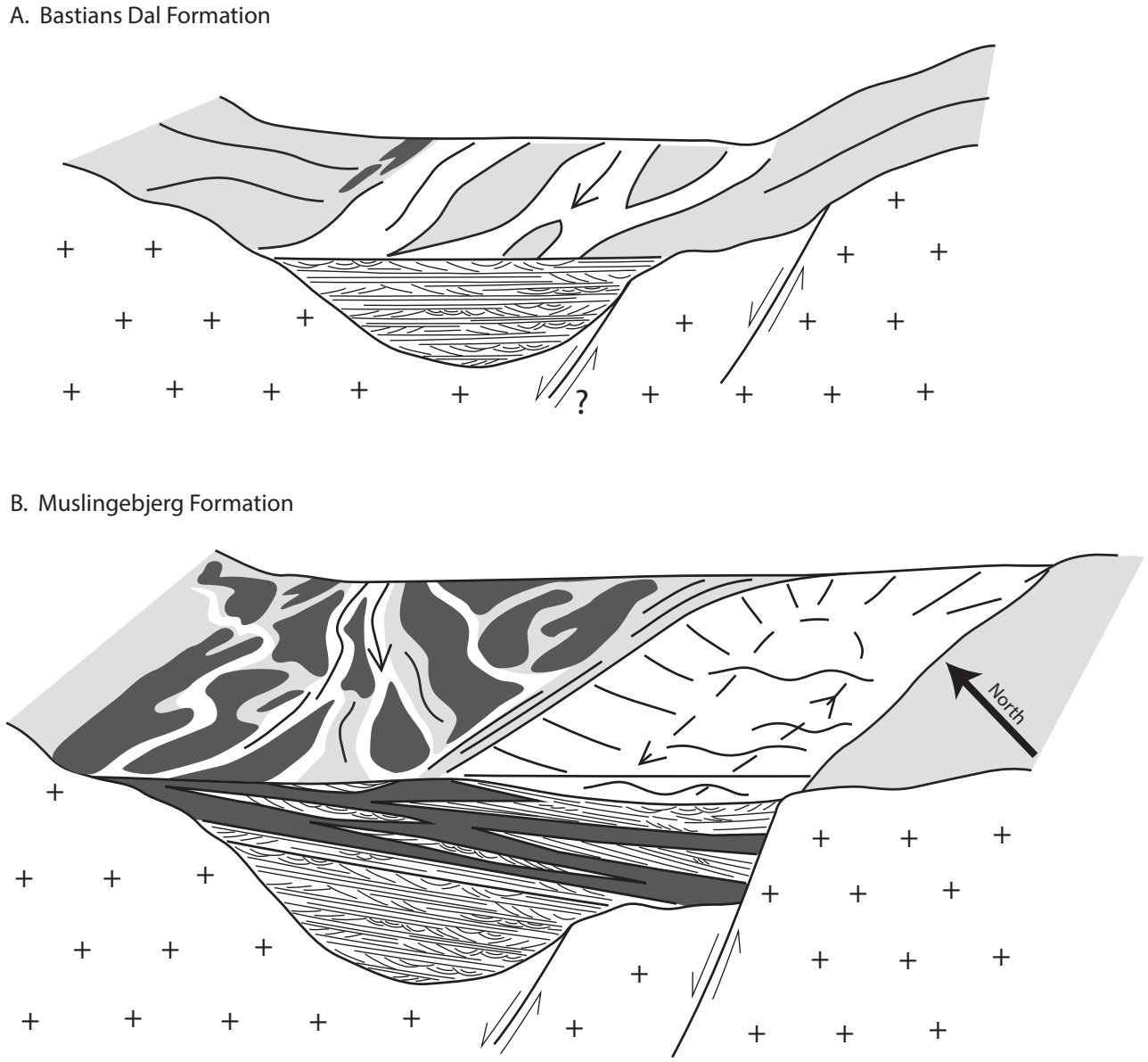

Fig. 13 Synthesis of sedimentological observations and stratigraphic geometries recorded in the Bastians Dal region. **(A)** Infilling valley that existed during the deposition of the Bastians Dal Formation. A gravel-bed fluvial system dominated deposition with finer-grained overbank facies becoming more common over time and including minor coal developments. The SW alignment of the valley may have been controlled by incipient faulting, which later also controlled the distribution of facies and stratal geometries within the Muslingebjerg Formation. Palaeoflow of the fluvial system is indicated by the **arrow**. **(B)** Interaction of environments recorded during the deposition of the Muslingebjerg Formation. Rising relative sea level and reduced topography in the hinterland led to widespread coal formation (**dark grey**). These were overlain by shallow-marine shoreface and tidal (**arrowed circulation**: dashed line) sandstones as sea level continued to rise. With continued regional transgression, the Muslingebjerg Formation gave way to the shallow-marine sandstones of the Pelion Formation (not shown). Palaeoflow of the fluvial system is indicated by the **thin arrow** (continuous line). As is clear from the stratal geometries described in this study, subsidence during this period was fault controlled. Legend for sedimentary structures in Figs 4 and 8.

coals are recognised towards the top of the Bastians Dal Formation, suggesting a transitional contact with the overlying Muslingebjerg Formation, the base of which is marked by the first thick coal. The Muslingebjerg Formation displays significant lateral variations in thickness as well as facies, thickening from a *c.* 5 m thick coal seam in the north to *c.* 50 m in the south (Fig. 13). The coals of the northern region of the study area contain minor intercalations of fluvial deposits, and these are replaced southwards with shoreface, and tidal facies associated with shallow-marine conditions (Fig. 13). These changing environments are also recorded in the coals, with a more humic character recorded in the north (Petersen *et al*. 2002), and, initially, more resinite-enriched coals in the south. Placed in a regional sequence stratigraphic context, the Muslingebjerg Formation appears to form part of a TST, where the overlying boundary to the Pelion Formation

represents regional marine flooding. Petersen *et al*. (2002) interpreted the coal-sandstone couplets of the Muslingebjerg Formation as higher-order sequences. Alternatively, these could be interpreted as sandstone-coal parasequences, comprising forestepping marine sandstones and associated coals deposited during the HST (e.g. Holz *et al*. 2002; Ketzer *et al*. 2003) and therefore genetically linked to the Pelion Formation.

Three coal samples and two sandstone samples were analysed for petroleum potential and oil staining. The samples are thermally immature, and none of the coal samples can be classified as oil-prone. However, recalculations of the properties of the live kerogen fraction based on the method of Dahl *et al*. (2004) suggest that sample 541232 is oil-prone, but that this feature is masked by a high concentration of 'dead' carbon. This is confirmed by the demonstration of bitumen-filled fractures in huminite macerals, probably caused by early generation from resinite – the more abundant among the generally sparse representatives of the liptinite maceral group. One of the sandstones is lightly stained by bitumen, indicated by both pyrolysis and microscopy. This was unexpected given the low level of thermal maturity of the coals and the associated problems of overcoming the expulsion threshold. Staining could possibly indicate the existence of intervals of higher resinite concentrations within the succession, where this threshold can be locally overcome.

The thickening of the Muslingebjerg formation is demonstrated to have been controlled by an NE–SW-oriented bounding fault in the south of the region. It seems likely that this also controlled the orientation of the underlying NE–SW-aligned palaeovalley. This is oblique to the proposed overall N–S orientation of faulting related to rifting through the Middle to Late Jurassic (Surlyk 2003; Guarnieri *et al*. 2017). Instead, these alignments resemble those of pre-Jurassic phases of rifting (Guarnieri *et al*. 2017; Andrews *et al*. 2021) and may therefore indicate a transitional phase of tectonism. Faulting on this alignment can be traced SW, aligning with the proposed Triassic fault of Guarnieri *et al.* (2017), which cuts Lindeman Fjord and follows the valleys east of the A. P. Olsen Land plateau.

Conclusions

The relationship between N–S oriented Jurassic rifting and earlier NE–SW-oriented Triassic rifting in East Greenland has received little attention. Deposits of Middle Jurassic age from central Kuhn Ø appear to demonstrate a continuity with Triassic structural trends, suggesting that a transition occurred during the Early to Middle Jurassic.

The south-westward flowing fluvial facies of the Bastians Dal Formation infill a NE–SW-oriented palaeovalley, the orientation of which may reflect incipient rifting. The overlying Muslingebjerg Formation is defined by the occurrence of coal, which is intercalated with both fluvial (in the north) and shallow marine facies (in the south). The coals are similar to those described elsewhere from the Muslingebjerg Formation but display subtle differences consistent with variable degrees of marine influence. A distinct NW–SE thickening of the Muslingebjerg formation is demonstrated to be controlled by a NE–SW-oriented fault.

The NE–SW orientation of palaeotopography, palaeocurrents and faulting identified in central Kuhn Ø is consistent with the orientation of Triassic rifting and can be traced SW to faulting that cuts across Lindeman Fjord and follows the valleys east of the A. P. Olsen Land plateau. To understand the geographic and temporal transition between the Triassic rifting and N–S-oriented Jurassic rifting, a detailed compilation of palaeocurrent data across this transition is required.

Acknowledgements

This work was undertaken during the Wollaston Forland regional mapping project, coordinated jointly by the Geological Survey of Denmark and Greenland (GEUS) and the Greenland Ministry of Industry, Energy, Research and Labour (MIERL). The authors would like to thank the editor, Mette Olivarius, and Tiffany Playter and Mihai Emilian Popa for their helpful reviews.

Additional information

Funding statement

This project was jointly funded by GEUS and MIERL.

Competing interests

The authors declare no competing interests.

Author contributions

SDA: field data collection, writing and conceptualisation. HV: field data collection, writing and manuscript editing. JAB-K: coal & bitumen analysis and writing.

Additional files

There are no supplementary files with this manuscript.

References

Ahokas, J.M., Nystuen, J.P. & Martinius, A.W. 2014: Depositional dynamics and sequence development in a tidally influenced marginal marine basin: Early Jurassic Neill Klinter Group, Jameson Land Basin, East Greenland. In: Stevens, T. (ed): From depositional systems to sedimentary successions on the Norwegian Continental Margin. International Association of Sedimentologists Special Publications **46**, 291–338. *https://doi.org/10.1002/9781118920435.ch12*

Alsgaard, P.C. *et al*. 2003: The Jurassic of Kuhn Ø, North-East Greenland. In: Ineson, J.R. & Surlyk, F. (eds): The Jurassic of Denmark and Greenland. Geological Survey of Denmark and Greenland Bulletin **1**, 865–892. *https://doi.org/10.34194/geusb.v1.4691*

Andrews, S.D., Morton, A.C. & Decou, A. 2021: Mid to Late Triassic evolution of the Jameson land Basin, East Greenland. Geological Magazine **158**(5), 930–949. *https://doi.org/10.1017/S001675682000093X*

Bojesen-Koefoed, J.A. *et al*. 2020: A mid-Cretaceous petroleum source-rock in the North Atlantic region? Implications of the Nanok-1 fully cored borehole, Hold with Hope, northeast Greenland Marine and Petroleum Geology **117**, 104414. *https://doi.org/10.1016/j.marpetgeo.2020.104414*

Bojesen-Koefoed, J.A. *et al*. 1996: Resinite-rich coals of northeast Greenland – A hitherto unrecognized, highly oil-prone Jurassic source rock. Bulletin of Canadian Petroleum Geology **44**(3), 458–473. *https://doi.org/10.35767/gscpgbull.44.3.458*

Bojesen-Koefoed, J.A. *et al*. 2012: A remote coal deposit revisited: Middle Jurassic coals at Kulhøj, western Germania Land, Northeast Greenland. International Journal of Coal Geology **98**, 50–61. *https://doi.org/10.1016/j.coal.2012.04.006*

Bordenave, M.L. *et al*. 1993: Chapter II-2: Screening techniques for source rock evaluation. In: Bordenave, M.L. (ed.): Applied petroleum geochemistry. pp. 219–278. Paris: Éditions Technip.

Clemmensen, L.B. & Surlyk, F. 1976: Upper Jurassic coal-bearing shoreline deposits, Hochstetter Forland, East Greenland. Sedimentary Geology **15**, 193–211. *https://doi.org/10.1016/0037-0738(76)90016-6*

Dahl, B. *et al*., 2004: A new approach to interpreting Rock-Eval S2 and TOC data for kerogen quality assessment. Organic Geochemistry **35**, 1461–1477. *https://doi.org/10.1016/j.orggeochem.2004.07.003*

Espitalié, J., Deroo, G. & Marquis, F., 1985: La pyrolyse Rock-Eval et ses applications. Première partie. Revue de l'institut Français du Pétrole **40**, 563–579. (In French)

Guarnieri, P., Brethes, A. & Rasmussen, T.M. 2017: Geometry and kinematics of the Triassic rift basin in Jameson Land (East Greenland). Tectonics **36**(4), 602–614. *https://doi.org/10.1002/2016TC004419*

Hartley, A.J. *et al*. 2015: Recognition and importance of amalgamated sandy meander belts in the continental rock record. Geology **43**(8), 679–682. *https://doi.org/10.1130/G36743.1*

Higgins, A.K. 2010: Exploration history and place names of northern East Greenland. GEUS Bulletin **21**, 1–368. *https://doi.org/10.34194/geusb.v21.4735*

Holz, M., Kalkreuth, W. & Banerjee, I. 2002: Sequence stratigraphy of paralic coal-bearing strata: an overview. International Journal of Coal Geology **48**(3–4), 147–179. *https://doi.org/10.1016/S0166-5162(01)00056-8*

Horn, G. 1931: Über Kohlen-Gerölle in Norwegen. Norsk Geologisk Tidsskrift **12**, 341–364. (In German)

Ketzer, J.M. *et al*. 2003: Sequence stratigraphic distribution of diagenetic alterations in coal-bearing, paralic sandstones: Evidence from the Rio Bonito Formation (early Permian), southern Brazil. Sedimentology **50**(5), 855–877. *https://doi.org/10.1046/j.1365-3091.2003.00586.x*

Khorasani, G.K. & Murchison, D.G. 1988: Order of generation of petroleum hydrocarbons from liptinitic macerals with increasing thermal maturity. Fuel **67**, 1160–1162. *https://doi.org/10.1016/0016-2361(88)90388-2*

Koch, L. & Haller, J. 1971: Geological map of East Greenland 72°–76° N. lat.(1: 250,000). Meddelelser om Grønland **183**, 26 pp. (13 maps)

Maync, W. 1947: Stratigraphie der Jurabildungen Ostgrönlands zwischen Hochstetterbugten (75°N) und dem Kejser Franz Joseph Fjord (73°N). Meddelelser om Grønland **132**(2), 223 pp. (In German)

Maync, W. 1949: The Cretaceous beds between Kuhn Island and Cape Franklin (Gauss Peninsula), northern East Greenland. Meddelelser om Grønland **133**(3), 291 pp.

Miall, A.D. 1996. The geology of fluvial deposits: sedimentary facies, basin analysis, and petroleum geology. 582 pp. Springer. *https://doi.org/10.1007/978-3-662-03237-4*

Petersen, H.I., Bojesen-Koefoed, J.A. & Nytoft, H.P. 2002. Source rock evaluation of Middle Jurassic coals, northeast Greenland, by artificial maturation: aspects of petroleum generation from coal. American Association of Petroleum Geologists Bulletin **86**, 233–256. *https://doi.org/10.1306/61EEDA9E-173E-11D7-8645000102C1865D*

Petersen, H.I. *et al*. 1998: Relative sea-level changes recorded by paralic liptinite-enriched coal facies cycles, Middle Jurassic Muslingebjerg Formation, Hochstetter Forland, Northeast Greenland. International Journal of Coal Geology **36**, 1–30. *https://doi.org/10.1016/S0166-5162(97)00032-3*

Petersen, H.I. *et al*. 2013: Unusual resinite-rich coals found in northeastern Greenland and along the Norwegian coast: Petrographic and geochemical composition. International Journal of Coal Geology **109–110**, 58–76. *https://doi.org/10.1016/j.coal.2013.02.001*

Petersen, H.I. & Vosgerau, H. 1999: Composition and organic maturity of Middle Jurassic coals, North-East Greenland: evidence for liptinite-induced suppression of huminite reflectance. International Journal of Coal Geology **41**, 257–274. *https://doi.org/10.1016/S0166-5162(99)00022-1*

Piasecki, S. & Stemmerik, L. 2004: Jurassic dinoflagellate cysts from Hochstetter Forland, North-East Greenland. In: Stemmerik, L. & Stouge, S. (eds): The Jurassic of North-East Greenland. Geological Survey of Denmark and Greenland Bulletin **5**, 89–97. *https://doi.org/10.34194/geusb.v5.4809*

Snowdon, L.R. 1991: Oil from Type-III organic matter: resinite revisited. Organic Geochemistry **17**, 741–747. *https://doi.org/10.1016/0146-6380(91)90018-F*

Snowdon, L.R. & Powell, T.G. 1982: Immature oil and condensate – modification of hydrocarbon generation model for terrestrial organic matter. American Association of Petroleum Geologists Bulletin **66**, 775–788. *https://doi.org/10.1306/03B5A313-16D1-11D7-8645000102C1865D*

Surlyk, F. 1977: Stratigraphy, tectonics and palaeogeography of the Jurassic sediments of the areas north of Kong Oscars Fjord, East Greenland. Bulletin Grønlands Geologiske Undersøgelse, **123**, 56 pp. *https://doi.org/10.34194/bullggu.v123.6665*

Surlyk, F. 1978: Submarine fan sedimentation along fault scarps on tilted fault blocks (Jurassic–Cretaceous boundary, East Greenland). Bulletin Grønlands Geologiske Undersøgelse **128**, 108 pp. *https://doi.org/10.34194/bullggu.v128.6670*

Surlyk, F. 1990: Timing, style and sedimentary evolution of Late Palaeozoic – Mesozoic extensional basins of East Greenland. In: Hardman, R.F.P. & Brooks, J. (eds): Tectonic events responsible for Britain's oil and gas reserves. Geological Society Special Publication (London) **55**, 107–125. *https://doi.org/10.1144/GSL.SP.1990.055.01.05*

Surlyk, F. 1991: Sequence stratigraphy of the Jurassic – lowermost Cretaceous of East Greenland. American Association of Petroleum Geologists Bulletin **75**, 1468–1488. *https://doi.org/10.1306/0C9B296B-1710-11D7-8645000102C1865D*

Surlyk, F., 2003: The Jurassic of East Greenland: a sedimentary record of thermal subsidence, onset and culmination of rifting. Geological Survey of Denmark and Greenland Bulletin **1**, 723–659. *https://doi.org/10.34194/geusb.v1.4688*

Surlyk, F. *et al*. 2021. Jurassic stratigraphy of East Greenland. GEUS Bulletin **46**, 6521. *https://doi.org/10.34194/geusb.v46.6521*

Surlyk, F. & Clemmensen, L.B. 1983: Rift propagation and eustacy as controlling factors during Jurassic inshore and shelf sedimentation in northern East Greenland. Sedimentary Geology **34**, 119–143. *https://doi.org/10.1016/0037-0738(83)90083-0*

Surlyk, F. & Ineson, J.R., 2003. The Jurassic of Denmark and Greenland: Key elements in the reconstruction of the North Atlantic Jurassic rift system. Geological Survey of Denmark and Greenland Bulletin **1**, 9–20. *https://doi.org/10.34194/geusb.v1.4644*

Surlyk, F. & Korstgård, J. 2013: Crestal unconformities on an exposed Jurassic tilted fault block, Wollaston Forland, East Greenland as an analogue for buried hydrocarbon traps. Marine and Petroleum Geology **44**, 82–95. *https://doi.org/10.1016/j.marpetgeo.2013.03.009*

Sørensen, E.V. & Dueholm, M. 2018: Analytical procedures for 3D mapping at the Photogeological Laboratory of the Geological Survey of Denmark and Greenland. Geological Survey of Denmark and Greenland Bulletin **41**, 99–104. *https://doi.org/10.34194/geusb.v41.4353*

Swan, A., Hartley, A.J., Owen, A. & Howell, J. 2018: Reconstruction of a sandy point-bar deposit: implications for fluvial facies analysis. In: Ghinassi, M., Columbera, L., Mountney, N.P., Reesink, A.J.H. & Bateman, M. (eds): Fluvial Meanders and Their Sedimentary Products in the Rock Record, 445–474. *https://doi.org/10.1002/9781119424437.ch17*

Taylor, G.H. *et al*. 1998: Organic Petrology. 704 pp. Berlin, Stuttgart: Gebrüder Borntraeger.

Vischer, A. 1943: Die postdevonische Tektonik von Ostgrönland zwischen 74° und 75°N. Br., Kuhn Ø, Wollaston Forland, Clavering Ø und angrenzende Gebiete. Meddelelser om Grønland **133**(1), 195 pp. (In German)

Vosgerau, H. *et al*. 2000: Forest fires, climate, and sea-level changes in a coastal plain – shallow marine succession (Early–Middle Oxfordian Jakobsstigen Formation, North-East Greenland). Journal of Sedimentary Research **70**, 408–418. *https://doi.org/10.1306/2DC40919-0E47-11D7-8643000102C1865D*